Cancer Chemother Pharmacol (2011) 68:465–475
DOI 10.1007/s00280-010-1502-y

ORIGINAL ARTICLE

Prediction of human pharmacokinetics and tissue distribution of apicidin, a potent histone deacetylase inhibitor, by physiologically based pharmacokinetic modeling

Beom Soo Shin · Jürgen B. Bulitta · Joseph P. Balthasar · Minki Kim · Yohan Choi · Sun Dong Yoo

Received: 6 June 2010 / Accepted: 26 October 2010 / Published online: 11 November 2010

Abstract
Purpose The objectives of this study were to develop physiologically based models for the pharmacokinetics (PK) and organ distribution of apicidin in rats and mice and to predict human PK in blood and organs.
Methods The PK of apicidin was characterized in rats and mice after i.v. bolus injection, and distribution to various tissues was determined in rats following i.v. infusions at steady state. The developed models were prospectively validated within rat and within mouse and by scaling from rat to mouse using data after multiple i.v. injections. Human PK was predicted by the physiologically based modeling using intrinsic clearance data for humans from in vitro experiments.
Results The Cl_s predicted for human (9.8 ml/min/kg) was lower than those found in mice (116.9 ml/min/kg) and rats (61.6 ml/min/kg), and the V_{ss} predicted for human (1.9 l/kg) was less than in mice (2.0 l/kg) and rats (2.5 l/kg). Consequently, the predicted $t_{1/2}$ was longer in human (2.3 h) than in mice and rats (0.4 and 0.9 h, respectively). The highest concentrations of apicidin were predicted in liver followed by adipose tissue, kidney, lung, spleen, heart, arterial blood, venous blood, small intestine, stomach, muscle, testis, and brain.
Conclusions The developed models adequately described the PK of apicidin in rats and mice and were applied to predict human PK. These models may be useful in predicting human blood and tissue concentrations of apicidin under different exposure conditions.

Keywords Apicidin · Pharmacokinetics · Tissue distribution · Physiologically based models · Human prediction

Introduction

Histone deacetylases and histone acetyl transferases are two types of enzymes involved in the modulation of chromatin structure and regulation of the cell cycle, including differentiation, proliferation, and apoptosis [1, 2]. Lately, the therapeutic potential for anti-proliferative activity has been reported for several histone deacetylase inhibitors, including suberoylanilide hydroxamic acid (SAHA) [3], depsipeptide [4], and apicidin [5]. Apicidin [cyclo(*N*–*O*-methyl-L-tryptophanyl-L-isoleucinyl-D-pipecolinyl-L-2-amino-8-oxodecanoyl)], a cyclic tetrapeptide isolated from the cultures of *Fusarium pallidoroseum*, is a potent histone deacetylase inhibitor that non-selectively induces histone hyperacetylation in parasites and mammals [6]. Apicidin has been shown to exhibit anti-proliferative activity against various cancer cell lines [7–10] and potential anticancer activity [11, 12]. The pharmacokinetics (PK) of apicidin in experimental animals have been previously reported by our

B. S. Shin
College of Pharmacy, Catholic University of Daegu, Gyeongsan-si, Gyeongbuk, Korea

J. B. Bulitta
Ordway Research Institute, Albany, NY, USA

J. P. Balthasar
Department of Pharmaceutical Sciences, School of Pharmacy and Pharmaceutical Sciences, State University of New York at Buffalo, Buffalo, NY, USA

M. Kim · Y. Choi · S. D. Yoo (✉)
School of Pharmacy, Sungkyunkwan University, 300 Cheoncheon-dong, Jangan-gu, Suwon, Gyeonggi-do 440-746, Korea
e-mail: sdyoo@skku.ac.kr

laboratory [13, 14], but no data are available on its PK in humans.

Drug development can greatly benefit from predictions of the PK in humans based on preclinical data. Human PK is commonly predicted by allometric scaling or by physiologically based pharmacokinetic (PBPK) modeling. Allometric scaling uses body size to scale clearance and volume of distribution from animals to man but does not account for specific tissue distribution data in animals. Refined methods for allometric scaling that incorporate brain weight, maximum lifespan potential and fractal concepts of drug disposition have been proposed [15, 16]. The PBPK modeling approach offers the advantage that information on physiological functions can be combined with drug-specific tissue penetration, plasma protein-binding and enzymatic activity data [17, 18]. PBPK modeling can also simultaneously use data from several animal species to predict PK in man [19]. Prospective validation studies are important to assure the predictive performance of a PBPK model from one tested species to another. The predictive performance can be assessed by comparing predicted and observed blood and tissue concentration profiles within one species or between different species. As especially tissue penetration data are often difficult or tedious to obtain in humans, prospective validation studies assessing the between-species scaling properties of a PBPK model based on two animal species offer an attractive alternative approach for early predictions of the PK and tissue distribution in humans.

The present study was conducted to (1) develop PBPK models that can describe the PK and tissue penetration of apicidin in rats and mice, (2) prospectively validate the predictive performance of the PBPK models by predicting mouse PK and tissue penetration using data from rat, and (3) predict human PK in blood and various tissues.

Materials and methods

Chemicals

Apicidin was prepared from *Fusarium sp*. strain KCTC 16677 according to a method described previously [20]. Trazodone, dimethylsulfoxide (DMSO), polyethylene glycol (PEG) 400, ketamine, xylazine, and ammonium acetate were purchased from Sigma (St. Louis, MO, USA). HPLC-grade acetonitrile, methanol, and *tert*-butyl methyl ether were purchased from J.T. Baker (Phillipsburg, NJ, USA). Ammonia water and ethanol were obtained from Yakuri Pure Chemicals (Osaka, Japan). Water was de-ionized prior to use by a Millipore Milli-Q water purification system (Milford, MA, USA).

Drug analysis

Apicidin concentrations were determined by a validated LC/MS/MS method reported previously [21]. The assay was linear over a range from 0.5 to 2,000 ng/ml ($r^2 > 0.9994$). The mean intra- and inter-day assay accuracy ranged from 99.9–101.5% to 94.8–102.1%, respectively, and the mean intra- and inter-day precision was between 2.7–5.9% and 1.6–11.5%, respectively.

Animals

Male Sprague–Dawley rats and male ICR mice (Jeil Animal Co., Ansung, Korea) were used in the study. Animals were kept in plastic cages with free access to standard diet (Samyang, Seoul, Korea) and water. The animals were maintained at a temperature of 22–24°C with a 12-h light–dark cycle and relative humidity of 50 ± 10%. Serum samples were harvested by centrifugation at 1,500×*g* for 10 min. Blood was allowed to clot for approximately 1 h before centrifugation to obtain serum. All samples, including homogenized tissue samples, were immediately frozen and stored at −20°C until analysis.

Determination of apicidin PK in rat serum after i.v. injection (dataset 1)

Rats (body weight 222–256 g, $n = 6$) were anesthetized by i.p. injection of ketamine and xylazine (90:10 mg/kg) and cannulated with a polyethylene tubing (0.58 mm i.d., 0.96 mm o.d, Natsume, Tokyo, Japan) in the jugular and femoral veins. After 2 days of recovery, apicidin dissolved in a mixture of DMSO:PEG 400:isotonic saline (15:65:20, v/v) was i.v. injected via the femoral vein (dose 1 mg/kg). Venous blood samples were collected prior to and at 5, 15, 30 min, 1, 1.5, 2, 3, 4, 6, and 8 h after injection, and serum was obtained by centrifugation.

Assessment of serum PK and tissue distribution in rats at steady state (dataset 2)

The extent of tissue distribution was determined in rats under steady-state conditions. Rats (230–270 g, $n = 10$) were cannulated as described above. After 2 days of recovery, apicidin dissolved in a mixture of DMSO:PEG 400:isotonic saline (15:65:20, v/v) was administered by simultaneous i.v. bolus injection (dose 0.52 mg/kg) and continuous infusion (rate 0.74 mg/h/kg) (Model 200 Infusion Pumps, KD Scientific, Boston, MA, USA). Blood samples were taken at 1, 2, 3, and 4 h after initiation of the infusion, and serum was obtained by centrifugation. At the end of the i.v. infusion, animals were humanely killed, and liver, adipose, testis, spleen, kidney,

muscle, small intestine, stomach, lung, heart, and brain were excised, blot dried, and homogenized (PowerGen 125, Fisher Scientific Co., Pittsburgh, PA, USA) in phosphate-buffered saline (pH 7.4). Tissue-to-blood partition ratios were calculated by converting serum concentrations to blood concentrations using the blood-to-serum partition ratios determined below. These ratios were calculated based on PK data after continuous infusion at steady state.

Blood-to-plasma partition coefficients in rat, mouse, and human

Apicidin was spiked to heparinized rat blood (10 ml), yielding a concentration of 500 ng/ml. After gentle mixing for 30 s, blood samples (2 ml each) were pipetted into borosilicate tubes. Each tube was placed in a water bath at 37°C and incubated by shaking at 60 rpm. Blood samples were taken at 0.5, 1, and 2 h after initiation of the incubation ($n = 4$ at each sampling time). Aliquots of the whole blood (50 µl) and plasma (100 µl) obtained by centrifugation at 1,500×g for 10 min were transferred to fresh borosilicate tubes. The blood-to-plasma partition coefficient was calculated as the average ratio of C_{blood}/C_{plasma}. The blood-to-plasma partition coefficients in mouse and human were also determined as described above. The blood-to-plasma partition coefficients were assumed to be identical to the blood-to-serum partition coefficients.

Strategy for development and prospective validation of PBPK models

The blood and tissue volumes and blood flow rates to each organ in rats, mice, and humans were obtained from the literature [22–24]. A PBPK model was developed for rats (Model I) (Fig. 1) using datasets 1 and 2 and validated using PK data in rats (dataset 3; see below). Before predicting the PK and tissue distribution of apicidin in man, a between-species validation was performed by predicting the PK and tissue distribution in mice. Model I was modified to predict the PK and tissue penetration in mice, since physiological data on the blood flows and tissue volumes of stomach, intestine, testis, and adipose tissue were not available for mouse. Specifically, Model I (that was based on rat data) was modified to develop a PBPK model that can predict the PK and tissue penetration in mouse using a lumped organ compartment (Model II). The volume of the lumped organ compartment in rat was calculated as the difference between total body weight and the sum of all other tissue weights. The blood-to-tissue partition coefficient of the lumped organ compartment in rat was estimated by model fitting using the observed blood concentrations in rats using dataset 1. To show that Models I and II yield similar predictions, serum and tissue concentration–time profiles simulated from Models I and II were compared. Parallel inter-species scaling was performed by predicting the serum and tissue concentrations in mice using Model II. After prospectively validating the

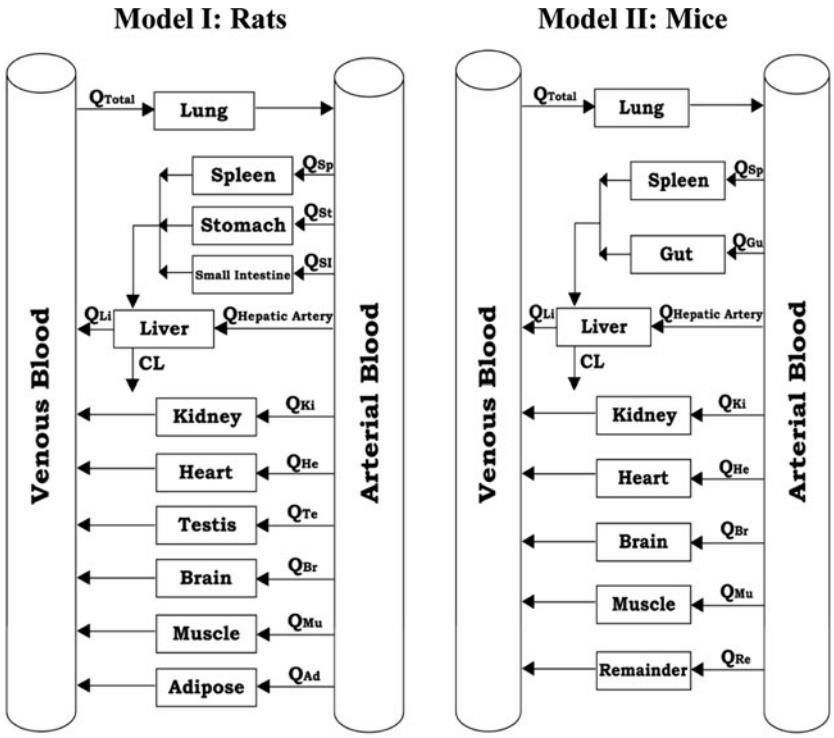

Fig. 1 PBPK models used to describe the pharmacokinetics of apicidin in rat, mouse, and human. Model II is a lumped space model used for the parallel inter-species scaling from rat to mouse

predictive performance of the proposed PBPK model, Model I was used to predict the PK and tissue penetration of apicidin in humans.

Development of PBPK model for rats—Model I

Model I includes compartments for venous and arterial blood and tissues, e.g., lung, spleen, liver, kidney, heart, testis, brain, muscle, adipose tissue, stomach, and small intestine (Fig. 1). Model I was developed using datasets 1 and 2. Differential equations that honor the mass balance principle were written for each component. Equation (1) applies to non-eliminating organs (spleen, stomach, small intestine, kidney, heart, testis, brain, muscle, and adipose tissue). Equation (2) applies to liver as the main eliminating organ, (3) to lung and (4) and (5) to venous and arterial blood. Liver was assumed to be the main eliminating organ as the amount of unchanged apicidin recovered in urine was negligible (<0.02%) [13]. The V and Q represent the organ volume and organ blood flow, respectively. The $Cl'_{int,Li}$ and f_u represent the hepatic intrinsic clearance of unbounded apicidin and unbound fraction of apicidin in blood, respectively. The abbreviations for the respective organ are indicated in parenthesis: vein (Ve), artery (Ar), lung (Lu), liver (Li), spleen (Sp), kidney (Ki), heart (He), testis (Te), brain (Br), muscle (Mu), adipose tissue (Ad), stomach (St), and small intestine (Si).

Differential equation for non-eliminating organs:

$$V_T\frac{dC_T}{dt} = Q_T C_{Ar} - Q_T\frac{C_T}{K_{P,T}} \quad (1)$$

Differential equation for an eliminating organ (liver; with $Q_{\text{Hepatic Artery}} = Q_{Li} - Q_{Sp} - Q_{St} - Q_{SI}$):

$$V_{Li}\frac{dC_{Li}}{dt} = Q_{\text{HepaticArtery}}C_{Ar} + Q_{Sp}\frac{C_{Sp}}{K_{Sp}} + Q_{St}\frac{C_{St}}{K_{St}} + Q_{SI}\frac{C_{SI}}{K_{SI}} - Q_{Li}\frac{C_{Li}}{K_{Li}} - f_u Cl'_{int,Li}\frac{C_{Li}}{K_{Li}} \quad (2)$$

for lung (with $Q_{Lu} = Q_{Total} = Q_{Ve}$):

$$V_{Lu}\frac{dC_{Lu}}{dt} = Q_{Lu}C_{Ve} - Q_{Lu}\frac{C_{Lu}}{K_{Lu}} \quad (3)$$

for venous blood:

$$V_{Ve}\frac{dC_{Ve}}{dt} = Q_{Li}\frac{C_{Li}}{K_{Li}} + Q_{Ki}\frac{C_{Ki}}{K_{Ki}} + Q_{He}\frac{C_{He}}{K_{He}} + Q_{Te}\frac{C_{Te}}{K_{Te}} + Q_{Br}\frac{C_{Br}}{K_{Br}} + Q_{Mu}\frac{C_{Mu}}{K_{Mu}} + Q_{Ad}\frac{C_{Ad}}{K_{Ad}} - Q_{Ve}C_{Ve} \quad (4)$$

for arterial blood:

$$V_{Ar}\frac{dC_{Ar}}{dt} = Q_{Lu}\frac{C_{Lu}}{K_{Lu}} - Q_{Ve}C_{ve} \quad (5)$$

Model II (lumped organ model)

A lumped organ PBPK model was developed to simulate the apicidin disposition in the mouse (Fig. 1). The stomach and intestine compartment were combined to the "gut" compartment, and the remainder compartment represents the sum of the testis and adipose tissue compartment (Fig. 1). The tissue-to-blood partition coefficient of the remainder compartment was estimated by model fitting between observed and simulated blood apicidin concentration vs. time profiles using dataset 1**.** Some of the differential equations described above are identical for the PBPK model in rats and the lumped organ model in mice: equation (1) applies to non-eliminating organs, (3) to lung and (5) to arterial blood. The differential equations for liver (as the main eliminating organ) and venous blood were:

Liver (with $Q_{\text{Hepatic Artery}} = Q_{Li} - Q_{Sp} - Q_{Gu}$):

$$V_{Li}\frac{dC_{Li}}{dt} = Q_{\text{HepaticArtery}}C_{Ar} + Q_{Sp}\frac{C_{Sp}}{K_{Sp}} + Q_{Gu}\frac{C_{Gu}}{K_{Gu}} - Q_{Li}\frac{C_{Li}}{K_{Li}} - f_u Cl'_{int,Li}\frac{C_{Li}}{K_{Li}} \quad (6)$$

venous blood:

$$V_{Ve}\frac{dC_{Ve}}{dt} = Q_{Li}\frac{C_{Li}}{K_{Li}} + Q_{Ki}\frac{C_{Ki}}{K_{Ki}} + Q_{He}\frac{C_{He}}{K_{He}} + Q_{Br}\frac{C_{Br}}{K_{Br}} + Q_{Mu}\frac{C_{Mu}}{K_{Mu}} + Q_{Re}\frac{C_{Re}}{K_{Re}} - Q_{Ve}C_{Ve} \quad (7)$$

where Gu represents gut and Re the remainder compartment.

Assessment of tissue-to-blood partition coefficients

Tissue-to-blood partition coefficients for the eliminating and non-eliminating organs were calculated by the following equations:

$K_{P,Li}$ for an eliminating organ (liver):

$$K_{P,Li} = \frac{C_{Li,SS}}{C_{B,SS}} \cdot \frac{Q_{Li} + f_u Cl'_{int,Li}}{Q_{Li}} \quad (8)$$

K_p for non-eliminating organs (all other tissues, T):

$$K_{P,T} = \frac{C_{T,SS}}{C_{B,SS}} \quad (9)$$

Validation of PBPK models in rats (dataset 3)

Rats (body weight 204–274 g, $n = 10$) were anesthetized by i.p. injection of ketamine and xylazine (90/10 mg/kg) and cannulated with a polyethylene tubing (0.58 mm i.d.; 0.96 mm o.d.; Natume, Tokyo, Japan) in jugular and femoral veins. After 2 days of recovery, apicidin dissolved in a mixture of DMSO:PEG 400:isotonic saline (15:65:20,

v/v) was given by multiple i.v. injections (0.5 mg/kg every 60 min) via the femoral vein. Blood samples were taken at 65, 75, 90, 105, 125, 130, 135, 150, 165, 185, 195, 210, 225, 245, 255, 285, and 305 min after initiation of multiple i.v. injections and centrifuged at 1,500×*g* for 10 min. Harvested serum samples were kept at −20°C until analysis.

In a separate study, rats were killed at 135, 185, 195, 245, 255, and 305 min after initiation of the multiple i.v. injections ($n = 1$–2 each), and lung, spleen, liver, kidney, heart, testis, brain, muscle, adipose tissue, stomach, and small intestine were excised. The tissue samples were homogenized as described above and kept at −20°C until analysis. For model validation, experimentally observed concentrations of apicidin in various tissues and blood were compared with simulated concentrations.

Validation of PBPK model for mice: parallel inter-species scaling (dataset 4)

The PBPK Model II was validated in mice after a single bolus i.v. injection (1 mg/kg) and after multiple i.v. injections (1 mg/kg every 30 min) of apicidin into the tail vein. After i.v. bolus injection, blood samples were taken by heart puncture at 5, 15, 30, 60, and 90 min ($n = 4$ per sampling time). Serum samples were obtained by centrifugation at 1,500×*g* for 10 min and kept at −20°C until analysis. After initiation of multiple i.v. injections, mice were killed at 65, 90, 125, and 155 min ($n = 4$ per sampling time), and blood and tissue samples were collected as described above. Harvested serum and tissue samples were kept at −20°C until analysis. For model validation, observed concentrations of apicidin in various tissues and blood were compared with simulated concentrations.

Prediction of human pharmacokinetics by PBPK modeling

Model I was used to predict the pharmacokinetics and tissue penetration of apicidin in humans after i.v. administration. Physiological and anatomical parameters of a 70-kg man were obtained from the literature [22–24]. Apicidin was assumed to be injected intravenously (dose 1 mg/kg). The hepatic clearance and blood-to-serum partition coefficients obtained previously in our laboratory were used for model fitting [14]. Concentration–time profiles of apicidin in blood and various body tissues were generated. In addition, pharmacokinetic parameters of the terminal half-life ($t_{1/2}$), systemic clearance (Cl_s), and the volume of distribution at steady state (V_{ss}) were calculated from the concentration–time profiles.

Data analysis

Computer fitting and simulations were achieved by using Scientist (Micromath Scientific Software, Salt Lake City, UT, USA). The partition coefficient of the lumped organ compartment was estimated using rat data. This estimate was used for parallel inter-species scaling from rat to mouse. Observed and predicted serum concentration–time data were analyzed by non-compartmental methods using WinNonlin (Scientific Consulting Inc., Cary, NC, USA). The goodness-of-fit was assessed by comparing the predicted and observed concentrations over time. The $t_{1/2}$, Cl_s, and V_{ss} were calculated using the linear trapezoidal rule extrapolated to infinite time using standard formulas implemented in WinNonlin.

Results

Pharmacokinetics of apicidin in rats and mice

Upon i.v. bolus injection (1 mg/kg) to rats and mice, serum concentrations of apicidin declined bi-exponentially. In agreement with allometric theory, half-life was shorter and clearance was slightly smaller in rats compared to mice, whereas volume of distribution in (l/kg) was comparable in both species (Table 1). Following simultaneous i.v. injection and continuous infusion to rats, steady-state serum concentrations were achieved within 2 h. As reflected by the K_p values (Table 2), the highest concentrations of apicidin at steady state were observed in liver followed by kidney, adipose tissue, spleen, lung, heart, small intestine, stomach, muscle, testis, and brain.

Application of PBPK models to rats

Physiological and drug-specific parameters of the organ blood flow rate, organ volume, and tissue-to-blood partition coefficients are shown in Table 2. Equilibrium of the blood-to-plasma partition for apicidin was achieved within 30 min of incubation. The average blood-to-plasma ratios were comparable in all three species (Table 2). The

Table 1 Pharmacokinetic parameters (mean ± SD) of apicidin in rats ($n = 6$) and mice ($n = 16$) determined after i.v. injection at a dose of 1 mg/kg

Animal	$t_{1/2}$ (h)	V_{ss} (l/kg)	Cl_s (ml/min/kg)
Rat	0.9 ± 0.2	2.5 ± 0.6	61.6 ± 16.6
Mouse	0.4	2.0	116.9

The pharmacokinetics parameter values for rat and mouse were obtained from the literature [13] and dataset 4, respectively

Table 2 Physiological and biochemical parameters used in the PBPK simulation for rat, mouse, and human

Organ	Rat		K_p[b]	Mouse		Human	
	Volume[a] (ml)	BF[a] (ml/min)		Volume[a] (ml)	BF[a] (ml/min)	Volume[a] (ml)	BF[a] (ml/min)
Venous blood	11.3	43.00	–	0.78	13.98	3,600	5,240
Arterial blood	5.6	43.00	–	0.20	13.98	1,800	5,240
Lung	1.0	43.00	1.26	0.18	13.98	1,170	5,240
Liver	10.3	11.80	69.72	1.37	2.25	1,690	1,650
Spleen	0.6	0.63	1.18	0.09	0.09	192	77
Kidney	2.3	9.23	1.70	0.42	1.27	310	1,100
Heart	0.8	3.92	1.02	0.13	0.92	267	150
Brain	1.7	1.33	0.07	0.41	0.46	1,450	700
Muscle	121.9	7.50	0.50	9.60	2.22	30,000	750
Gut	8.7	7.52	0.89	1.06	1.50	1,650	1,100
Testis	2.5	0.45	0.30	NA	NA	36	2.4
Adipose	10.0	0.40	1.37	NA	NA	10,000	260
Stomach	1.1	1.14	0.87	NA	NA	155	39
Remainder[c]	–	–	0.18[f]	10.77[d]	5.26[e]	–	–
Biochemical parameter							
Blood-to-serum ratio		0.70		0.64		0.68	
$f_u Cl'_{int,Li}$ (ml/min)[g]		8.6		1.9		284.2	

BF blood flow; K_p partition coefficient

[a] Values were taken from literature [22–24]

[b] K_p values were calculated by (8)–(9)

[c] Remainder values were used for Model II in place of sum of testis, adipose, and stomach

[d] Calculated as the difference between total body weight and sum of other tissue weights

[e] Calculated as the difference between cardiac output and the sum of blood flow to sampled tissues

[f] Calculated by model fitting between observed and simulated blood apicidin concentration vs. time profiles in rats. The partition coefficients (K_p) were assumed to be the same in all three species. The K_p for the remainder compartment was only used for Model II to obtain predictions in mice

[g] Values were taken from literature [14]

intrinsic hepatic clearances reported in literature are listed in Table 2. The observed and model-predicted concentrations of apicidin in blood and various tissues in rats after multiple i.v. injections agreed well (Fig. 2). The highest concentrations of apicidin were found in liver followed by kidney, adipose tissue, spleen heart, lung, stomach, small intestine, blood, muscle, testis, and brain.

Application of PBPK models to mice

Model II was initially developed to predict the pharmacokinetics of apicidin in mouse. The estimated blood-to-tissue partition coefficient for the remainder compartment was 0.18 (Table 2). To assure that Models I and II yield similar predictions, we simulated the concentration–time profiles in blood and all tissues common to both models for an i.v. bolus administration. The ratio of concentrations simulated from models from 0 to 360 min was 0.99 [0.85–1.15] (median [range]). This indicates that both models yielded virtually identical predictions for the time course of concentrations in blood and the tissues common to both models.

Application of PBPK model to mice: parallel inter-species scaling

The observed and predicted concentration–time profiles in blood and tissues using Model II agreed well after multiple i.v. injections (Fig. 3). The highest steady-state concentration of apicidin was found in liver followed by kidney, spleen, lung, gut, heart, blood, muscle, remainder, and brain. The blood pharmacokinetic parameters obtained from simulated and observed profiles were comparable. The non-compartmental PK parameters calculated from the simulated vs. observed concentration–time profiles were 0.4 versus 0.4 h for $t_{1/2}$, 100 versus 117 ml/min/kg for Cl_s, and 2.1 versus 2.0 l/kg for V_{ss}.

The model development and model validation strategy to obtain adequate predictions for humans is summarized in Fig. 4. Model I was developed and validated using data in

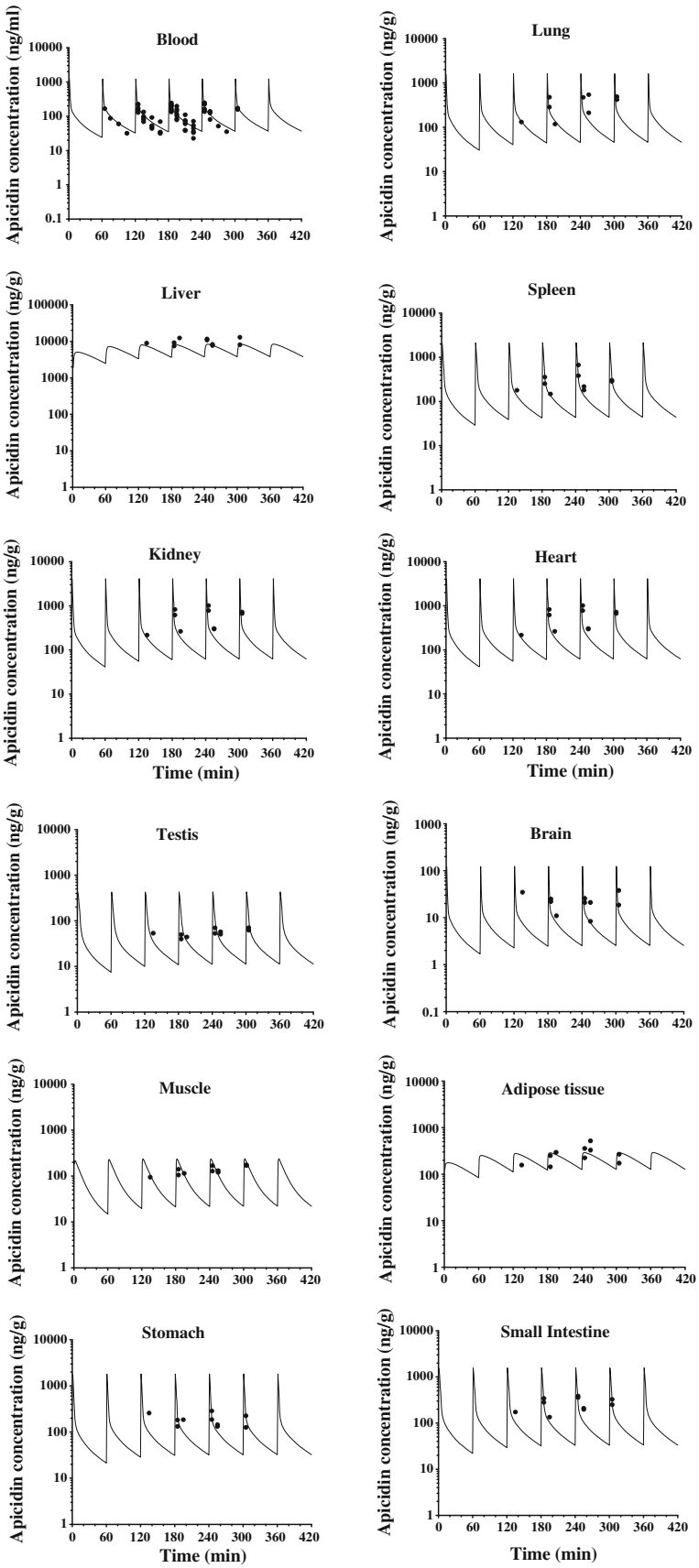

Fig. 2 Predicted (*solid line*) and observed (*filled circle*) concentrations of apicidin in blood, lung, liver, spleen, kidney, heart testis, brain, muscle, adipose, stomach, and small intestine after multiple i.v. injections to rats (dose 0.5 mg/kg; dataset 3). These data were used to validate Model I by comparing observed and predicted concentrations of apicidin in blood and various tissues

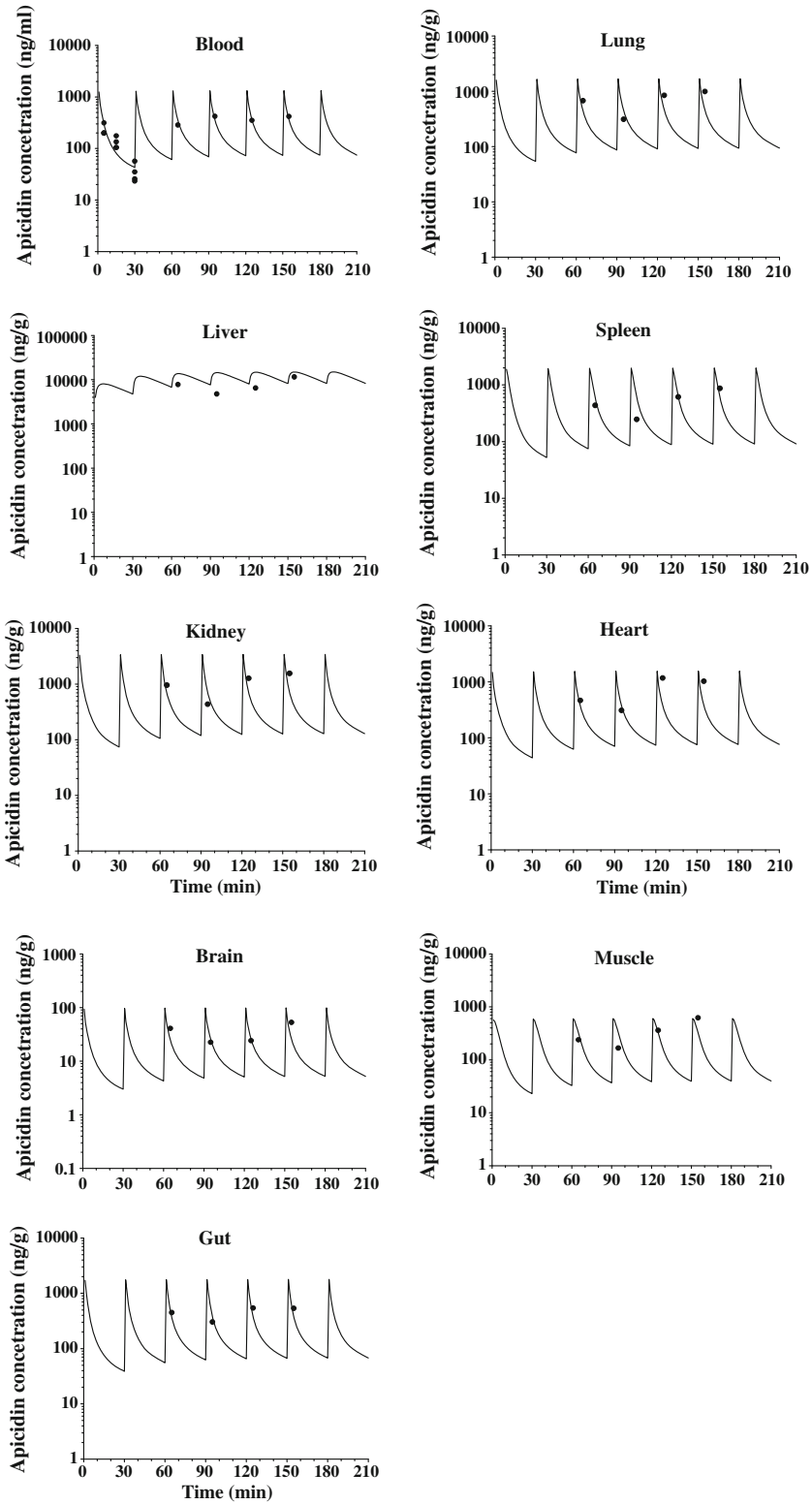

Fig. 3 Predicted (*solid line*) and observed (*filled circle*) concentrations of apicidin in blood, lung, liver, spleen, kidney, heart, brain, muscle, gut, and the remainder compartment after multiple i.v. injections to mice (dose 1 mg/kg; dataset 4). These data were used to validate Model II

rats. Then Model II was developed to obtain predictions in mice using a lumped organ approach. Models I and II yielded essentially identical predictions for blood and all organs common to both models, and these predictions were in good agreement with experimentally observed data in mice. After this series of validation steps, Model I was used to predict the PK in blood and tissues in humans.

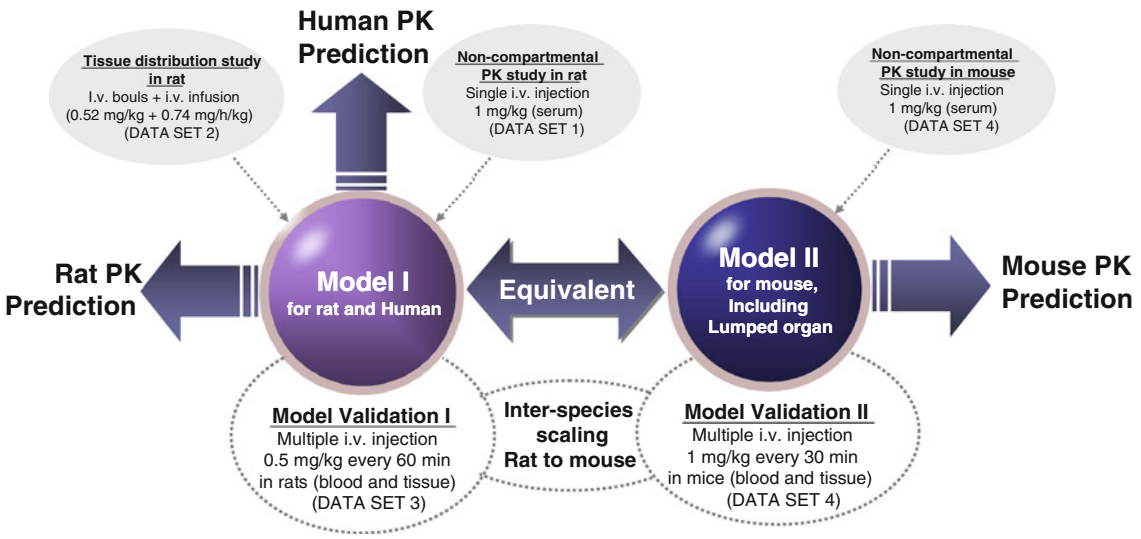

Fig. 4 Model development and model validation strategy to assure adequate predictions of the PK in blood and tissues in humans

Prediction of human pharmacokinetics

Figure 5 represents the concentration vs. time courses of apicidin in blood and organs of human simulated by Model I. During the terminal phase, apicidin concentrations in blood and organs declined in parallel. The highest concentrations of apicidin were predicted in liver followed by adipose tissue, kidney, lung, spleen, heart, arterial blood, venous blood, small intestine, stomach, muscle, testis and brain. The predicted $t_{1/2}$ was 2.3 h in human, which was longer than those in mice and rats (0.4 and 0.9 h; Table 2). The Cl_s predicted for human (9.8 ml/min/kg) was lower than those found in mice (116.9 ml/min/kg) and rats (61.6 ml/min/kg). The V_{ss} predicted for human (1.9 l/kg) was less than in mice (2.0 l/kg) and rats (2.5 l/kg).

Discussion

An important application of PBPK modeling is inter-species prediction of tissue concentration–time profiles in humans based on animal data. Concentration–time profiles of specific target organs can be predicted by adding the target organ as a compartment in the PBPK model. This methodology is important for predicting the potential toxicity of a drug in preclinical development. Adding a target

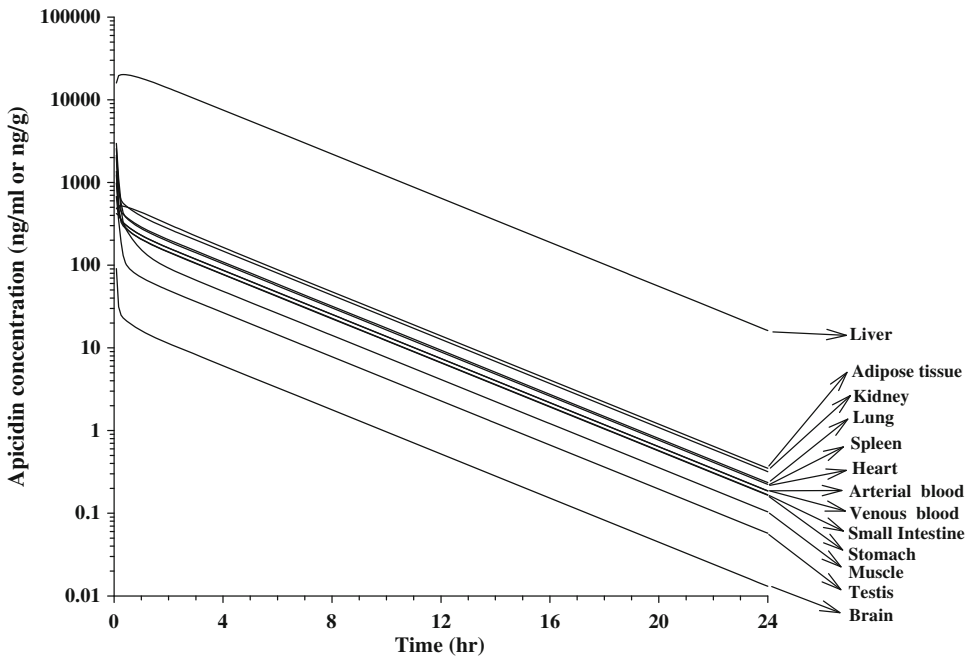

Fig. 5 Simulated time courses of apicidin concentration in blood and organs in a 70-kg human after i.v. injection (1 mg/kg dose)

organ compartment is the opposite process of lumping organs, which is used for simplifying the structure of a PBPK model. Both processes, adding and lumping, have been referred to as the PBPK model reconstruction [17]. The PK of a potential drug can alternatively be predicted via quantitative structure PK relationships [25]. This method presents an appealing in silico technique that does not require synthesizing the compound of interest. We applied a PBPK modeling approach, since PBPK modeling has the advantage that PK data from animals are used as prior information to predict the PK in humans. These prior data should improve the accuracy of the model predictions for humans.

Our PBPK modeling strategy (Fig. 4) included model development and validation in rats and development of a slightly modified model for mice (Fig. 2). Model II was used to predict the pharmacokinetics of apicidin in the mouse as no reported literature values were available for the blood flow to stomach, testis, and adipose tissue in this species. Accordingly, a remainder compartment incorporating these tissues was added to this model (Model II). Then, the PK in mice was successfully predicted via parallel inter-species scaling. This between-species comparison (Fig. 3) added credibility to our predictions in humans. A potential limitation of our study is the lack of data on the PK in a primate species, for example. While such data would have added more credibility to our predictions in humans, the extensive validation within rats (Fig. 2) and the between-species validation from rats to mice (Fig. 3) in the present study yield a sufficient degree of confidence for initial predictions of the PK in humans.

Inter-species scaling is a common application of PBPK modeling. It is critically important to assure the predictive performance of a model via prospective validation studies. Such model validation is commonly performed by comparing predicted and observed blood and tissue concentration–time profiles in a tested species. The predicted blood and tissue apicidin concentration–time profiles for multiple i.v. injections in mice showed good agreements with the observed profiles (Fig. 3). Also, the pharmacokinetic parameter values for $t_{1/2}$, Cl_s, and V_{ss} calculated from the predicted or observed concentrations were comparable. Thus, the downward inter-species scaling from rat to mouse was successfully achieved.

Our data characterized the complete concentration–time profile of apicidin in rat blood (Fig. 2). While the PK in blood characterized the terminal phase well, we focused on characterizing the drug exposure in tissues. Therefore, more observations were collected during early time points for the PK in tissue, and fewer samples were collected during the terminal phase in tissues (Fig. 3). Therefore, this approach is expected to characterize the PK and exposure (area under the curve) in tissue well and relies on the common assumption that concentrations decline in parallel in blood and tissue during the terminal phase. This assumption is common to all linear PK models. The K_p values were determined experimentally at steady state for each tissue in rats. Therefore, this approach is embedded in literature data and leaves only a minor extent of flexibility from estimating model parameters. After successfully predicting the PK and tissue penetration in rats and predicting the PK and tissue penetration from rats to mice, the proposed PBPK model appears to be sufficiently validated to obtain initial predictions for the PK in humans. The human pharmacokinetic disposition was predicted using Model I. Upon single i.v. injection, apicidin levels in blood and organs were predicted to decline in parallel with each other. During the terminal elimination phase, apicidin levels were predicted to be highest in liver followed by adipose tissue, kidney, and lung.

In summary, this study examined the pharmacokinetics of apicidin in rats and mice after single and multiple i.v. injections. PBPK models were developed to describe the pharmacokinetic disposition of apicidin in these animals and to predict the blood pharmacokinetics and tissue distribution characteristics in human. The developed PBPK models were prospectively validated by parallel interspecies scaling from rats to mice. Our modeling predicted that the highest concentrations in humans are expected in liver followed by adipose tissue, kidney, and lung. These models may be useful in predicting human blood and tissue concentrations of apicidin under different exposure conditions.

Acknowledgments This work was supported in part by the National Research Foundation (NRF) grant (2009-0083962) and the National Research Foundation of Korea (NRF) grant funded by the Korea government (MEST) (No. 2010-0022780).

References

1. Marks PA, Richon VM, Rifkind RA (2000) Histone deacetylase inhibitors: inducers of differentiation or apoptosis of transformed cells. J Natl Cancer Inst 92:1210–1216
2. Meinke PT, Liberator P (2001) Histone deacetylase: a target for antiproliferative and antiprotozoal agents. Curr Med Chem 8:211–235
3. Marks PA, Richon VM, Rifkind RA (2000) Histone deacetylase inhibitors: inducers of differentiation or apoptosis of transformed cells. J Natl Cancer Inst 92:1210–1216
4. Konstantinopoulos PA, Vandoros GP, Papavassiliou AG (2006) FK228 (depsipeptide): a HDAC inhibitor with pleitropic antitumor activities. Cancer Chemother Pharmacol 58:711–715
5. Krämer OH, Göttlicher M, Heinzel T (2001) Histone deacetylase as a therapeutic target. Trends Endocrin Metab 12:294–300
6. Darkin-Rattray SJ, Gurnett AM, Myers RW, Dulski PM, Crumley TM, Allocco JJ, Cannova C, Meinke PT, Colletti SL, Bednarek MA, Singh SB, Goetz MA, Dombrowski AW, Polishook JD, Schmatz DM (1996) Apicidin: a novel antiprotozoal agent that inhibits parasite histone deacetylase. Proc Natl Acad Sci USA 93:13143–13147

7. Han JW, Ahn SH, Park SH, Wang SY, Bae GU, Seo DW, Kwon HK, Hong S, Lee HY, Lee YW, Lee HW (2000) Apicidin, a histone deacetylase inhibitor, inhibits proliferation of tumor cells via induction of p21WAF1/Cip1 and Gelsolin1. Cancer Res 60:6068–6074
8. Kwon SH, Ahn SH, Kim YK, Bae GU, Yoon JW, Hong S, Lee HY, Lee YW, Lee HW, Han JW (2002) Apicidin, a histone deacetylase inhibitor, induces apoptosis and Fas/Fas ligand expression in human acute promyelocytic leukemia cells. J Biol Chem 277:2073–2080
9. Park H, Im JY, Kim J, Choi WS, Kim HS (2008) Effects of apicidin, a histone deacetylase inhibitor, on the regulation of apoptosis in H-ras-transformed breast epithelial cells. Int J Mol Med 21:325–333
10. Noh JH, Song JH, Eun JW, Kim JK, Jung KH, Bae HJ, Xie HJ, Ryu JC, Ahn YM, Wee SJ, Park WS, Lee JY, Nam SW (2009) Systemic cell-cycle suppression by apicidin, a histone deacetylase inhibitor, in MDA-MB-435 cells. Int J Mol Med 24:205–226
11. Kim SH, Ahn S, Han JW, Lee HW, Lee HY, Lee YW, Kim MR, Kim KW, Kim WB, Hong S (2004) Apicidin is a histone deacetylase inhibitor with anti-invasive and anti-angiogenic potentials. Biochem Biophys Res Commun 315:964–970
12. Pluemsampant S, Safronova OS, Nakahama K, Morita I (2008) Protein kinase CK2 is a key activator of histone deacetylase in hypoxia-associated tumors. Int J Cancer 122:333–341
13. Shin BS, Chang HS, Park EH, Yoon CH, Kim HY, Kim J, Ryu JK, Zee OP, Lee KC, Cao D, Yoo SD (2006) Pharmacokinetics of a novel histone deacetylase inhibitor, apicidin, in rats. Biopharm Drug Dispos 27:69–75
14. Shin BS, Park EH, Yoon CH, Kim J, Zee OP, Yoo SD (2005) In vitro investigation of the hepatic intrinsic clearance of apicidin, a histone deacetylase inhibitor, in mouse, rat, and human with correlation by nonspecific protein binding. J Toxicol Environ Health A 68:2207–2218
15. Mahmood I (2009) Pharmacokinetic allometric scaling of antibodies: application to the first-in-human dose estimation. J Pharm Sci 98:3850–3861
16. Karalis V, Claret L, Iliadis A, Macheras P (2001) Fractal volume of drug distribution: it scales proportionally to body mass. Pharm Res 18:1056–1060
17. Nestorov IA, Aarons LJ, Arundel PA, Rowland M (1998) Lumping of whole-body physiologically based pharmacokinetic models. J Pharmacokinet Biopharm 26:21–46
18. Meno-Tetang GML, Li H, Mis S, Pyszczynski N, Heining P, Lowe P, Jusko WJ (2006) Physiologically based pharmacokinetic modeling of FTY720 (2-amino-2[2-(-4-octylphenyl)ethyl]propane-1, 3-diol hydrochloride) in rats after oral and intravenous doses. Drug Metab Dispos 34:1480–1487
19. Ruelius HW (1987) Extrapolation from animals to man: predictions, pitfalls and perspectives. Xenobiotica 17:255–265
20. Park JS, Lee KR, Kim JC, Lim SH, Seo JA, Lee YW (1999) A hemorrhagic factor (apicidin) produced by toxic Fusarium isolates from soybean seeds. Appl Environ Microbiol 65:126–130
21. Shin BS, Kim J, Yoon CH, Kim CH, Park EH, Han JW, Yoo SD (2005) Development of a liquid chromatography/electrospray tandem mass spectrometry assay for the quantification of apicidin, a novel histone deacetylase inhibitor, in rat serum: application to a pharmacokinetic study. Rapid Commun Mass Spectrom 19:408–414
22. Bernareggi A, Rowland M (1991) Physiologic modeling of cyclosporin kinetics in rat and man. J Pharmacokinet Biopharm 19:21–50
23. Brown RP, Delp MD, Lindstedt SL, Rhomberg LR, Beliles RP (1997) Physiological parameter values for physiologically based pharmacokinetic models. Toxicol Ind Health 13:407–484
24. Davies B, Morris T (1993) Physiological parameters in laboratory animals and humans. Pharm Res 10:1093–1095
25. Mager DE (2006) Quantitative structure-pharmacokinetic/pharmacodynamic relationships. Adv Drug Deliv Rev 58:1326–1356